On the role of Al-Si ordering in the cubic-tetragonal phase transition of leucite

Martin T. Dove, Tracey Cool, David C. Palmer, Andrew Putnis,
Ekhard K. H. Salje, Björn Winkler*

Department of Earth Sciences, University of Cambridge, Downing Street, Cambridge CB2 3EQ, U.K.

Abstract

The cubic-tetragonal phase transition in leucite has been examined using static lattice energy calculations with realistic, tested interatomic potentials. The calculations have demonstrated that the transition is not triggered by Al-Si ordering and can occur without any ordering. Any Al-Si order will have only a minor effect on the observed spontaneous strain and structure distortion. Calculations show that any long-range Al-Si order is associated with the energetics of next-nearest Al-O-Al linkages rather than nearest neighbor interactions, leading to a low ordering temperature.

Introduction

Leucite ($KAlSi_2O_6$) undergoes a cubic-tetragonal phase transition at 938 K. The high- and low-temperature phases have the space groups $Ia3d$ and $I4_1/a$, respectively. An intermediate tetragonal phase with the space group $I4_1/acd$ is stable over the range 918–938 K (Grögel et al., 1984; Lange et al., 1986; Palmer et al., 1989, 1990). The structure refinements of the cubic (Peacor, 1968) and room-temperature tetragonal (Mazzi et al., 1976) phases show that the Si and Al atoms occupy tetrahedral sites. However, in the cubic structure there is only one independent tetrahedral site, implying that there is no long-range site ordering of the Al and Si atoms in this phase. In the two tetragonal structures there are two ($I4_1/acd$) and three ($I4_1/a$) nonequivalent tetrahedral sites, so in principle long-range Al-Si site ordering is possible. There is disagreement over the role of Al-Si ordering in the cubic-tetragonal phase transition in leucite. Hatch et al. (1990) considered the ordering to be the driving mechanism of the transition and took the degree of ordering to be equivalent to the order parameter of the transition. In this model the changes in structure and the spontaneous strain arise from the fact that the two cations are of different size, so that the Al and Si sites distort the framework in different ways. On the other hand, Palmer and Salje (1990) have argued that the transition is too rapid to be caused by Al-Si ordering, and that the primary instability is due to a displacive mechanism independent of any Al-Si ordering. However, some degree of short-range order is indicated by the NMR studies of Brown et al. (1987), Murdoch et al. (1988), and Phillips et al. (1989). In view of these uncertainties, which experiments appear to be unable to clarify, we have chosen to determine the significance of the role of Al-Si ordering in the mechanism of the phase transitions in leucite by using lattice energy calculations.

Lattice energy calculations are an ideal tool for investigations of crystal stability, providing that a well-tested, reliable model is available. Such a model is available and has recently been tested on a wide range of aluminosilicate minerals (Winkler et al., 1991; Patel et al., 1991). These tests were sufficiently comprehensive that we have a very good knowledge of the limits of reliability of the model, which is essential when using modeling as a predictive tool. The purpose of this paper, therefore, is to use lattice energy calculations to identify the role of Al-Si site ordering, if there is one, in the cubic-tetragonal phase transition in leucite and to calculate the effects of ordering on the spontaneous strains. We also present calculations on the energetics of long-range ordering.

Model Calculations

The empirical model used in the present lattice energy calculations was originally developed by Sanders et al. (1984) and Price et al. (1987) and has been fully described by Winkler et al. (1991). The basic model uses short-range Born-Mayer interactions for Al-O and K-O (parameters taken from Catlow et al., 1982, and Post and Burnham, 1986) and Buckingham interactions for Si-O and O-O (parameters taken from Sanders et al., 1984). Formal charges have been assumed for the Coulomb interactions, and a shell model is used to account for the polarizability of the O atoms (parameters from Sanders et al., 1984, and Winkler et al., 1991). Covalent effects are accounted for by use of a bond-bending potential for O-Si-O and O-Al-O bonds (parameters from Sanders et al., 1984). The complete set of parameters for the model are given in Winkler et al. (1991). These authors tested the model against a number of mineral structures and thereby demonstrated that it can be successfully applied to a wide range of aluminosilicate structures. It was found that unit-cell edge lengths were reproduced to within 2%, bond lengths to better than 2% for Si-O or Al-O bonds and to better than 4% for all other cation-O contact distances, O-Si-O and O-Al-O bond angles to within 2°, and

---

bond orientations for all cation-O contacts to within 2.5°. More important than being able simply to reproduce crystal structures, it was also found that the model could correctly predict the *P-T* slopes of phase boundaries, excess volumes, and enthalpies associated with deviations from ideal behavior in solid solutions, the magnitudes of spontaneous strains associated with Al-Si order-disorder phase transitions, phonon frequencies, and basic thermodynamic functions. Winkler et al. (1991) were able to conclude that the model is fully transferable and, within the limits of error given above, can be used as a reliable predictive tool.

Winkler et al. (1991) described a pragmatic scheme for calculating effective potentials for disordered sites, aimed at obtaining the correct effects on the long-range structure. The effective potentials are obtained by equating the first and second differentials of the effective potential with the weighted means of the corresponding differentials of the Si-O and Al-O potentials evaluated at the observed bond length (or mean bond length). This leads to a pair of equations for the Born-Mayer repulsive interaction; the dispersive and Coulomb terms are trivially obtained. This scheme has been used in the present study, taking the average bond lengths for the tetragonal structure (as given later in Table 6). The effective potentials will not give the correct energies for a disordered structure; for that more sophisticated methods (Jones et al., 1990) or supercell methods (Bertram et al., 1990) are required. For our purposes the effective potentials constructed by the method of Winkler et al. (1991) are quite adequate for modeling the structures (as opposed to energetics) of disordered phases.

The program used for the lattice energy calculations was THBREL,[1] which uses a standard minimization technique to find the lowest energy structure, namely that for which there are no internal or external stresses. THBREL does not impose any symmetry constraints on the structure relaxation and effectively treats any structure as triclinic P1. The only constraint is on the number of atoms in the unit cell. Therefore the minimization can cause a relaxation of the structure into a lower symmetry polymorph if that leads to a lowering of the lattice energy. We find that only in exceptional cases (small unit cells with high symmetry) is special care required to avoid false, high-symmetry minima. THBREL allows for relaxation under conditions of constant volume, in which only the coordinates of the atoms within a unit cell of fixed size and shape can change, and constant pressure, in which the unit cell parameters can also change in the minimization procedure.

We note that lattice energy calculations do not include the effects of lattice vibrations and technically correspond

---

[1] The program THBREL used in this study is supported by CCP5 SERC, Daresbury Laboratory, Warrington, Cheshire WA4 4AD, U.K. The program has not been fully described in the scientific literature; a brief description of the main features is given in Winkler et al. (1991).

TABLE 1. The unit-cell parameters of leucite and the spontaneous strains

	Observed	Disordered	Order model 1	Order model 2
a (Å)	13.090	12.988	12.931	13.005
c (Å)	13.753	13.800	13.812	13.765
a_0 (Å)	13.480	13.644	13.644	13.644
$\bar{a}_0$ (Å)	13.311	13.259	13.225	13.258
e_a	0.0127	0.0290	0.0317	0.0291
e_e	0.0332	0.0408	0.0444	0.0382

Note: All quantities are defined in the text (Eqs. 3–5). The experimental data are from Palmer et al. (in preparation). The tetragonal cell parameters were measured at 300 K, and the cubic cell parameter was measured at 970 K.

to simulating classical crystals at $T = 0$ K. Although the effects of thermal expansion are therefore neglected in the comparison with experimental data obtained at nonzero temperatures, the errors in such calculations from the model interatomic potentials are usually larger than the effects of thermal expansion.

CRYSTAL STRUCTURES AND ORDER PARAMETERS

The unit-cell parameters and atomic fractional coordinates of leucite in both the high-temperature cubic ($Ia3d$) and room-temperature tetragonal ($I4_1/a$) phases that have been determined from neutron diffraction data (Palmer et al., in preparation) are given in Tables 1–3.

Phase transitions in which the symmetry of the low-symmetry phase is a subgroup of that of the high-symmetry phase can be characterized by an order parameter, which describes the amplitude of the distortion of the structure from its high symmetry form (Bruce and Cowley, 1981). The distortions of a crystal structure that undergoes a displacive phase transition can generally be described by a single normal mode of the high-symmetry structure, which becomes a static distortion in the low-symmetry phase. The order parameter in this case is given by the static amplitude of this normal mode. Although the different atoms in the crystal may move by different amounts in different directions, it is generally found that the basic distortion pattern is the same for all temperatures; temperature only modifies the overall amplitude (the order parameter). Each order parameter can therefore be defined as the change in fractional coordinates of the atoms through the distortion from the high-symmetry phase to the low-symmetry phase. The effects of thermal expansion, or even spontaneous strains, will lead to only small high-order corrections to these definitions.

In the case of leucite, we expect that there will be two order parameters, corresponding to the two point-group symmetry changes $m\bar{3}m \rightarrow 4/mmm$ (E_g representation of $m\bar{3}m$) and $4/mmm \rightarrow 4/m$ (A_{2g} representation of $4/mmm$). We consider here only the O atoms. The positions of the O atoms are described by three independent coordinates in the cubic phase (Table 2), nine in the intermediate tetragonal phase, and 18 in the low-symmetry tetragonal phase (Table 3). These coordinates can be transformed to highlight their relation in the higher symmetry phases;

TABLE 2. Crystal structure data for cubic leucite

	Observed	Calculated
a (Å)	13.536	13.644
K x	⅜	⅜
K y	⅜	⅜
K z	⅛	⅛
T x	0.0878	0.0878
T y	⅜	⅜
T z	0.1622	0.1623
O x	0.1329	0.1354
O y	0.2807	0.2813
O z	0.1034	0.1035

Note: The crystal setting used the space-group generators x, y, z; ½ + x, ½ + y, ½ + z; $-x, -y, -z$; ¾ − y, ¼ + x, ¼ + z; ½ + y, z, ½ + x. The experimental data are from Palmer et al. (in preparation) and were obtained at 970 K.

TABLE 3. The fractional atomic coordinates for tetragonal leucite

	Observed	Disordered	Order model 1	Order model 2
K x	0.3663	0.3660	0.3713	0.3618
K y	0.3654	0.3631	0.3568	0.3619
K z	0.1171	0.1073	0.1129	0.1197
T1 x	0.0582	0.0563	0.0556	0.0564
T1 y	0.3967	0.3971	0.3960	0.3982
T1 z	0.1654	0.1671	0.1681	0.1672
T2 x	0.1685	0.1668	0.1698	0.1671
T2 y	0.6124	0.6115	0.6098	0.6134
T2 z	0.1280	0.1269	0.1267	0.1283
T3 x	0.3933	0.3929	0.3978	0.3926
T3 y	0.6406	0.6407	0.6361	0.6413
T3 z	0.0863	0.0848	0.0844	0.0861
O1 x	0.1308	0.1327	0.1296	0.1352
O1 y	0.3136	0.3162	0.3154	0.3168
O1 z	0.1111	0.1097	0.1097	0.1117
O2 x	0.0927	0.0881	0.0867	0.0902
O2 y	0.5105	0.5135	0.5076	0.5159
O2 z	0.1310	0.1329	0.1328	0.1330
O3 x	0.1455	0.1459	0.1429	0.1471
O3 y	0.6790	0.6819	0.6857	0.6816
O3 z	0.2269	0.2257	0.2281	0.2284
O4 x	0.1342	0.1325	0.1299	0.1352
O4 y	0.6839	0.6857	0.6868	0.6887
O4 z	0.0358	0.0359	0.0320	0.0388
O5 x	0.2892	0.2894	0.2994	0.2898
O5 y	0.5773	0.5733	0.5700	0.5758
O5 z	0.1212	0.1183	0.1183	0.1209
O6 x	0.4841	0.4839	0.4899	0.4838
O6 y	0.6175	0.6161	0.6167	0.6175
O6 z	0.1665	0.1659	0.1636	0.1663

Note: The calculated values were obtained using the three models described in the text. The crystal setting used the space-group generators x, y, z; ½ + x, ½ + y, ½ + z; $-x, -y, -z$; ¾ − y, ¼ + x, ¼ + z. The experimental data are from Palmer et al. (in preparation), and were obtained at 300 K.

these transformations are given in Table 4. We call the transformations reduced coordinates. In the intermediate phase, pairs of reduced coordinates have identical values, i.e.,

$$u_{i,j} = u_{7-i,j} \tag{1}$$

where the subscript i denotes the atom and the subscript j denotes the component (x, y, or z) of the position. In the high-temperature phase we have only three independent coordinates:

$$u_{1,j} = u_{2,j} = u_{3,j} = u_{4,j} = u_{5,j} = u_{6,j} = w_j \tag{2}$$

where w_j is the mean of u_{ij} (averaged over all atoms i) in the low-symmetry phase. Thus we can define the individual order parameters P_{ij} (for the transition $Ia3d \rightarrow I4_1/acd$) and Q_{ij} (for the transition $I4_1/acd \rightarrow I4_1/a$) as given in Table 4. Each of these parameters gives the relative motion of each atom as part of the overall symmetry-breaking distortion; the relative motions are then scaled by the overall amplitude given by the order parameter. The temperature dependence of these order parameters has recently been determined (Dove, 1990) using the structural data of Palmer et al. (in preparation). Similar order parameters can be defined for the tetrahedral sites and the K atoms, but their values are smaller than for O. In order not to encumber the reader with too much detail, we only consider the O order parameters here.

LATTICE ENERGY CALCULATIONS FOR TETRAGONAL LEUCITE

Fully disordered leucite

A fully disordered model is obtained by using the same effective interactions for each tetrahedral site. Whereas this model excludes any effects of short-range order, it does allow us to focus on the inherent displacive component of the phase transition. The tetragonal $I4_1/a$ structure of leucite could easily be relaxed in the lattice energy minimization calculation, since it is the stable structure at low temperature. The results are given in Tables 1 and 3. On the other hand, the cubic structure could not be relaxed so easily because it is unstable with respect to the tetragonal modification. We therefore carried out a num-

ber of constant-volume energy minimizations for the cubic structure using a range of cubic unit-cell lengths. The strain-free unit-cell length was obtained by fitting a fourth-order polynomial to the results, and finding the minimum of this function. A final constant-volume structure relaxation of the cubic phase with this value of the unit-cell length was carried out; the results of this calculation confirmed that the relaxed structure was free of all residual external stresses. The results are given in Tables 2 and 3. We did not attempt to model the intermediate phase, since this is unstable with respect to the low-temperature phase, but the distortions from the cubic phase associated with the intermediate modification are present in the calculated structure of the low-temperature phase.

The calculated cell parameters and structures of the tetragonal and cubic phases of leucite are compared with experimental data in Tables 1–3, and the calculated values of the microscopic order parameters are given in Table 5. It is clear from the results that the model has reproduced the main features of the structures, including the distortions associated with the phase transition. In particular, the model has correctly reproduced the sizes of the order parameters.

The distortions of the structure are accompanied by large spontaneous strains, which are the main signatures of the phase transition. Palmer et al. (1989) have defined two strain components, a volume-changing strain, e_a, and

TABLE 4. Definition of the order parameters associated with the displacive phase transition in leucite for the O atoms

Reduced coordinates*

$u_{11} = x_1$	$u_{12} = y_1$	$u_{13} = z_1$
$u_{21} = \frac{1}{4} - z_2$	$u_{22} = \frac{3}{4} - y_2$	$u_{23} = \frac{1}{4} - x_2$
$u_{31} = y_3 - \frac{1}{2}$	$u_{32} = \frac{1}{2} - z_3$	$u_{33} = x_3$
$u_{41} = \frac{1}{4} - x_4$	$u_{42} = \frac{1}{4} + z_4$	$u_{43} = \frac{3}{4} - y_4$
$u_{51} = z_5$	$u_{52} = x_5$	$u_{53} = y_5 - \frac{1}{2}$
$u_{61} = \frac{3}{4} - y_6$	$u_{62} = \frac{3}{4} - x_6$	$u_{63} = \frac{1}{4} - z_6$

Mean coordinates**

$$w_j = \frac{1}{6} \sum_{i=1}^{6} u_{ij}$$

Order parameters

$la3d \rightarrow I4_1/acd$: $\quad P_{ij} = w_j - (u_{ij} + u_{7-i,j})/2; \quad P_s = \left[\sum_{i,j} P_{ij}^2 \right]^{1/2}$

$I4_1/acd \rightarrow I4_1/a$: $\quad Q_{ij} = (u_{ij} - u_{7-i,j})/2; \quad Q_s = \left[\sum_{i,j} Q_{ij}^2 \right]^{1/2}$

Note: The subscript i denotes the atom, and the subscript j denotes the x, y, or z component of the coordinates. The definitions of the reduced coordinates have been chosen to give the most compact formalism for the definitions of the order parameters.
* Where x_i, y_i, z_i are the fractional coordinates of the ith O atom.
** Note that the fractional coordinates for the O atom in the cubic phase are equivalent to (w_1, w_2, w_3).

TABLE 5. Calculated and observed values of the O order parameters in leucite

	Observed	Disordered	Order model 1	Order model 2
		$la3d \rightarrow I4_1/acd$		
P_{11}	1.1	0.3	2.7	−0.2
P_{12}	−12.0	−13.1	−9.2	−13.6
P_{13}	9.2	9.6	7.9	8.9
P_{21}	14.1	15.8	16.2	14.7
P_{22}	13.1	15.1	7.6	15.9
P_{23}	−10.4	−11.1	−10.7	−11.2
P_{31}	−15.2	−16.1	−18.9	−14.6
P_{32}	−1.1	−2.0	~1.6	−2.3
P_{33}	1.2	1.4	2.9	2.3
P_s	30.7	33.6	30.9	32.9
		$I4_1/acd \rightarrow I4_1/a$		
Q_{11}	−1.2	−0.6	−0.6	−1.9
Q_{12}	24.0	25.1	27.7	25.3
Q_{13}	13.4	12.8	11.6	14.0
Q_{21}	−1.5	−0.6	−0.6	−1.9
Q_{22}	−25.3	−26.4	−28.5	−27.8
Q_{23}	41.3	44.3	46.6	42.0
Q_{31}	30.3	32.2	32.8	33.4
Q_{32}	−6.4	−5.8	−5.0	−8.6
Q_{33}	40.4	40.8	39.9	42.9
Q_s	75.5	78.7	81.1	80.1

Note: The values have been multiplied by 10^4.

a ferroelastic strain, e_e:

$$e_a = \frac{a_0 - \tilde{a}_o}{\tilde{a}_o} \tag{3}$$

$$e_c = \frac{c - \tilde{a}_o}{\tilde{a}_o} \tag{4}$$

where a and c are the tetragonal unit-cell lengths, a_0 is the cubic unit-cell length as extrapolated to low temperatures, and $\tilde{a}_o$ is given by

$$\tilde{a}_o = \frac{c + 2a}{3} \tag{5}$$

($\tilde{a}_o$ would be equal to a_0 if the transition were purely ferroelastic, i.e., $e_a = 0$). The behavior of these strains has been discussed in some detail by Palmer et al. (1989). The calculated spontaneous strains are compared with the experimental values in Table 1, taking the value of a_0 from the energy minimization of the cubic structure. The calculated value of the ferroelastic strain, e_c, is in reasonable agreement with experiment, but the calculations have overestimated the size of e_a by a factor of 2. That is because the calculated unit-cell length, a_0, differs from the experimentally determined value (discrepancy of 1.2%) by more than the differences between any of the other calculated and observed unit-cell lengths. One possible origin of this discrepancy is the existence of orientational disorder of the tetrahedra in the cubic phase, which will tend to shorten the actual cell length, but which cannot be included in the calculation (Dove et al., 1993). In the calculation of the strains, small errors in the individual cell parameters are magnified when calculating small differences between two large quantities.

The differences between the calculations and the experimental data do not affect the unequivocal conclusion that the model that treats each tetrahedral site equivalently has reproduced the main features of the cubic-tetragonal phase transition in leucite. The significance of this conclusion is that it shows that Al-Si ordering is not required at all for the phase transition to occur and that the mechanism of the transition is completely separate from the question of Al-Si ordering. We would like to stress that the errors in the calculated cell parameters of the tetragonal phase (0.8 and 0.3%) are much smaller than the difference between a and c (5%), so the conclusion from our calculations is well within the accuracy of the calculation.

The structures of hypothetical ordered phases

We performed additional lattice energy minimization calculations of leucite with two Al-Si ordering schemes. In model 1 we placed Al on the tetrahedral site T2 and Si on the remaining tetrahedral sites—this corresponds to a fully ordered structure with no Al-O-Al linkages and with the same symmetry as the observed tetragonal phase. Model 2 used effective potentials corresponding to the Al-Si distribution assigned from the results of the ^{27}Al NMR study of leucite by Phillips et al. (1989), namely that the site T1 contains 50% Al and 50% Si and that the sites T2 and T3 both contain 25% Al and 75% Si. The results of both models for the cell parameters, structures, and order parameters are given in Tables 1, 3, and 5.

It can be seen from the results of Table 1 that any Al-Si ordering has only a small effect on the spontaneous strains. The additional strains due to Al-Si ordering are similar in magnitude to the small strains induced by Al-Si ordering in cordierite (Putnis et al., 1987; Winkler et al., 1991). The calculations indicate that >95% of the observed strain in the leucite structure at room temper-

TABLE 6. Comparison of calculated T-O bond lengths with observed values

	Observed (Å)	Disordered (Å)	Order model 1 (Å)	Order model 2 (Å)
T1-O1	1.626	1.647	1.629	1.660
T1-O2	1.649	1.645	1.625	1.658
T1-O2	1.626	1.637	1.576	1.661
T1-O3	1.667	1.654	1.590	1.683
Mean T1-O	1.642	1.646	1.605	1.666
T2-O2	1.664	1.635	1.705	1.616
T2-O3	1.644	1.664	1.745	1.659
T2-O4	1.638	1.644	1.723	1.627
T2-O5	1.648	1.672	1.757	1.672
Mean T2-O	1.649	1.654	1.733	1.644
T3-O3	1.645	1.659	1.592	1.645
T3-O5	1.665	1.669	1.602	1.656
T3-O6	1.649	1.658	1.637	1.650
T3-O6	1.675	1.666	1.653	1.658
Mean T3-O	1.658	1.663	1.621	1.652

ature is independent of the degree of Al-Si long-range order. It is also seen from Table 5 that the ordering has little effect on the sizes of the order parameters from the displacive part of the transition. It therefore appears that there is only a weak coupling between the ordering and the displacive transition. The lack of an apparent systematic effect of the ordering on the values of the order parameters suggests that the coupling between the displacive and order-disorder transitions has a nontrivial form, which is not surprising, given that the effective sizes of the tetrahedra will change. This implies that higher order terms are as significant as the lower order terms in the corresponding free energy expansion (Salje, 1990).

Bond lengths

The tetrahedral bond lengths in the tetragonal structures calculated by the different models are compared with experimental data in Table 6. The best agreement with the experimental bond lengths is obtained with the fully disordered model. The sites with the excess of Al in the ordered models have significantly longer bond lengths. This comparison suggests that there is no significant long-range Al-Si order in leucite. Our own neutron diffraction studies of leucite, in which the site occupancies are treated as refinable parameters (Palmer et al., in preparation), do not indicate the existence of significant long-range order. We did find, however, that the values of the site occupancies were strongly correlated with other parameters in the structure refinements, suggesting that it would in any case be difficult to confirm the existence of long-range order from refinements of site occupancies alone.

ENERGETICS OF Al-Si ORDERING

Bragg-Williams treatment

We now consider the question of why long-range Al-Si ordering is apparently not observed in natural samples of leucite. Let us first take the simplest case of ordering, namely Al on T2 and Si on T1 and T3. This ordering scheme does not lower the symmetry of the tetragonal

$I4_1/a$ structure, and there are no Al-O-Al linkages (note that the only linkages are T1-O-T1, T1-O-T2, T3-O-T2, and T3-O-T3). The simplest Bragg-Williams type of mean field treatment of this model, which assumes that only nearest neighbor interactions are important and that configurational entropy is the only important contribution to the entropy, gives an expression for the excess free energy, ΔG, of ordering:

$$\Delta G = \frac{RT}{3}[4(1 - \eta)\ln(1 - \eta) + (1 + 2\eta)\ln(1 + 2\eta)$$

$$+ 4(1 + \eta/2)\ln(1 + \eta/2)] - \frac{2V\eta^2}{3} \quad (6)$$

where V is the energy for the reaction (Al-O-Al + Si-O-Si) → 2(Al-O-Si). The value of V is not known experimentally for leucite, but it can reasonably be supposed that it will not be very different from that for cordierite, namely 34 kJ/mol (Carpenter et al., 1983). The symbol η is the order parameter for this ordering, defined as

$$\eta = (3n - 1)/2 \quad (7)$$

where n is the average number of Al atoms on a T2 site (equal to 1 for a fully ordered structure, and equal to ⅓ in a completely disordered structure).

The expression for the free energy of ordering predicts a second-order phase transition at the temperature T_c, obtained as the temperature at which both the first and second differentials of ΔG with respect to η equal 0 (the point at which the free energy function changes from having a minimum at $\eta = 0$ to a maximum):

$$T_c = \frac{4V}{9R}. \quad (8)$$

Using the value of V determined for cordierite leads to a prediction for the value of T_c of around 1800 K. This result is subject to considerable uncertainty because of the error in the value of V and in the approximations inherent in the Bragg-Williams model, but it will nevertheless be of the correct order of magnitude. We therefore predict that if this actual ordering occurs, it produces a phase transition at a temperature that is high enough to be observed, particularly as this predicted ordering transition temperature is similar to Al-Si ordering transition temperatures in other aluminosilicate minerals (Carpenter, 1988). One might therefore expect to be able to observe this ordering experimentally, if it did in fact occur.

Lattice energy calculations and the value of the ordering energy

We next examine the energetics of ordering predicted by our potential model, principally to confirm that there is nothing anomalous about the value of V used in the Bragg-Williams model. For this we used a cubic unit cell fixed at the volume calculated in the previous section—we chose this lattice because we are interested in ordering from the disordered cubic phase. We performed energy minimization experiments with a number of different
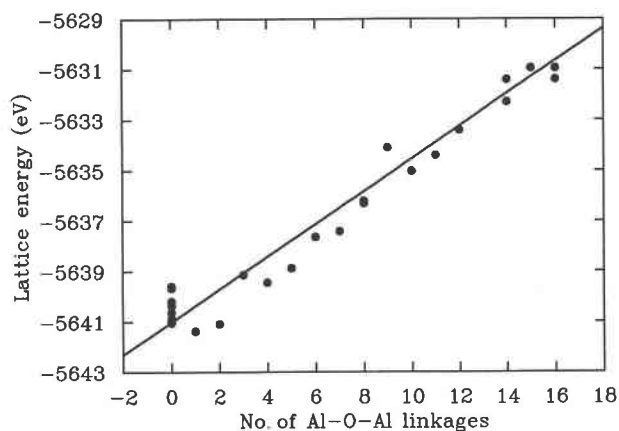
Fig. 1. Energy of disordered configurations of leucite as a function of the number of Al-O-Al linkages per unit cell (16 formula units). We present the absolute energies, which are given in electron volts for ease of labeling.
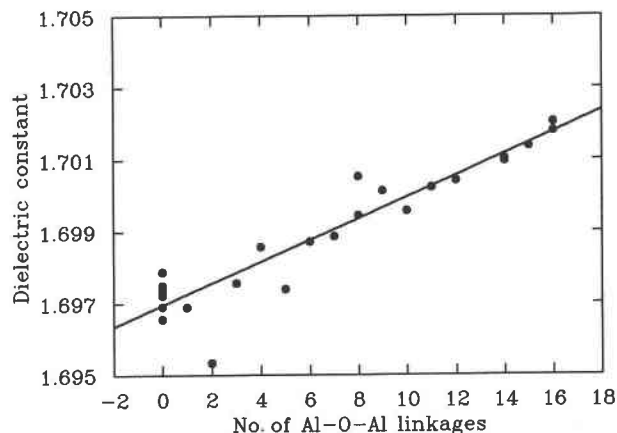

Fig. 2. High-frequency dielectric constant of disordered leucite as a function of the number of Al-O-Al linkages per unit cell (16 formula units).

configurations of the Al and Si atoms (the total number of atoms in one cubic cell is 32 Si and 16 Al), giving a range of numbers of Al-O-Al linkages in a single configuration. This approach is similar to that used in a recent study of the energetics of Al-Si ordering in sillimanite (Bertram et al., 1990). It was found that there is a good linear relationship between the energy of the configuration and the number of Al-O-Al linkages—the fitted straight line is shown in Figure 1, and the standard deviation of the calculated energies from the fitted line is 0.9 eV for a range in values of energy of 11 eV. From the gradient of the graph we deduce a value of $V = 0.65 \pm 0.03$ eV $= 63 \pm 3$ kJ/mol. This value is larger than the experimental value for cordierite, but it falls between the values of 54 and 94 kJ/mol obtained for sillimanite for Al-Al distances of 2.9 and 3.2 Å, respectively (Bertram et al., 1990—the Al-Al distance for leucite is 3.1 Å). The disagreement with the cordierite value is probably due to inadequacies with the potential model, which was developed without including any information about energy. However, we can still conclude that the value of V in leucite is not anomalously low.

In passing we draw attention to the correlation shown in Figure 2, namely that the high-frequency dielectric constant (and hence the refractive index) of the cubic phase of leucite depends on the number of Al-O-Al linkages. This observation could be of interest for the characterization of disordered minerals with different degrees of short-range order, although calculations on other systems would be of some value.

Why is the ordering temperature so low?

Given that there is nothing anomalous about the energetics of ordering in leucite, we finally address the question of why the temperature of the phase transition for Al-Si ordering is so low. We believe that the problem of ordering in leucite is associated with the fact that it is possible to produce disordered configurations that have no Al-O-Al linkages; this is due to the relatively high ratio (2:1) of Si to Al atoms in the structure. We have calculated the energy of seven configurations of disordered leucite with no Al-O-Al linkages and have obtained a standard deviation of the energy of 58 kJ/mol. This is slightly smaller than the value of V. It is therefore clear that it is energetically favorable for the disordered phase of leucite to have no Al-O-Al linkages; therefore the energy associated with Al-O-Al linkages does not provide a driving force for ordering. A similar situation appears to occur in albite (Post and Burnham, 1987). In that case the Al-Si ordering occurs at a much lower temperature than a displacive phase transition (Salje et al., 1985) and is partly assisted by the distortions associated with the displacive phase transition (Post and Burnham, 1987). This is unlike the case of sillimanite (Bertram et al., 1990), where the high transition temperature is determined by energy of Al-O-Al linkages. We surmise that in leucite the transition temperature for Al-Si ordering will be either below the transition temperature for the displacive phase transition or not greatly above it, although with the present calculations we are not able to demonstrate which. If the ordering transition temperature is below that for the displacive phase transition, then the ordering energy is affected by the displacive transition, and so calculations of the ordering energy need to be performed using the tetragonal structure rather than the cubic structure used here.

REFERENCES CITED

Bertram, U.C., Heine, V., Leslie, M., and Price, G.D. (1990) Computer modeling of Al/Si ordering in sillimanite. Physics and Chemistry of Minerals, 17, 326–333.

Brown, I.W.M., Cardile, C.M., MacKenzie, K.J.D., Ryan, M.J., and Meinhold, R.H. (1987) Natural and synthetic leucites studied by solid state 29-Si and 27-Al NMR and 57-Fe Mössbauer spectroscopy. Physics and Chemistry of Minerals, 15, 78–83.

Bruce, A.D., and Cowley, R.A. (1981) Structural phase transitions, 326 p. Taylor and Francis, London.

Carpenter, M.A. (1988) Thermochemistry of aluminium/silicon ordering in feldspar minerals. In E.K.H. Salje, Ed., Physical properties and thermodynamic behaviour of minerals, p. 265–323. Reidel, Dordrecht, The Netherlands.

Carpenter, M.A., Putnis, A., Navrotsky, A., and McConnell, J.D.C. (1983) Enthalpy effects associated with Al,Si ordering in anhydrous Mg cordierite. Geochimica et Cosmochimica Acta, 47, 899–906.

Catlow, C.R.A., Mackrodt, J.R., and Stewart, R.F. (1982) Defect energies in aluminium oxide and rutile titanium oxide. Physical Review B, 25, 1006–1026.

Dove, M.T. (1990) Phase transitions in minerals. ISIS annual report, p. 41–46. Rutherford Appleton Laboratory, U.K.

Dove, M.T., Giddy, A.P., and Heine, V. (1993) Rigid unit mode model of displacive phase transitions in framework silicates. Transactions of the American Crystallographic Association, 27, in press.

Grögel, T., Boysen, H., and Frey, F. (1984) Phase transition and ordering in leucite (abs.). Acta Crystallographica A, 40S, C256–C257.

Hatch, D.M., Ghose, S., and Stokes, H.T. (1990) Phase transitions in leucite, KAlSi$_2$O$_6$. I. Symmetry analysis with order parameter treatment and the resulting microscopic distortions. Physics and Chemistry of Minerals, 17, 220–227.

Jones, I.L., Heine, V., Leslie, M., and Price, G.D. (1990) A new approach to simulating disorder in crystals. Physics and Chemistry of Minerals, 17, 238–245.

Lange, R.A., Carmichael, I.S.E., and Stebbins, J.F. (1986) Phase transitions in leucite (KAlSi$_2$O$_6$), orthorhombic KAlSiO$_4$, and their iron analogues (KFeSi$_2$O$_6$, KFeSiO$_4$). American Mineralogist, 71, 937–945.

Mazzi, F., Galli, E., and Gottardi, G. (1976) The crystal structure of tetragonal leucite. American Mineralogist, 61, 108–115.

Murdoch, J.B., Stebbins, J.F., Carmichael, I.S.E., and Pines, A. (1988) A silicon-29 nuclear magnetic resonance study of silicon-aluminium ordering in leucite and analcite. Physics and Chemistry of Minerals, 15, 370–382.

Palmer, D.C., and Salje, E.K.H. (1990) Phase transitions in leucite: Dielectric properties and transition mechanism. Physics and Chemistry of Minerals, 17, 444–452.

Palmer, D.C., Salje, E.K.H., and Schmahl, W.W. (1989) Phase transitions in leucite: X-ray diffraction studies. Physics and Chemistry of Minerals, 16, 714–719.

Palmer, D.C., Bismayer, U., and Salje, E.K.H. (1990) Phase transitions in leucite: Order parameter behaviour and the Landau potential deduced from Raman spectroscopy and birefringence studies. Physics and Chemistry of Minerals, 17, 259–265.

Patel, A., Price, G.D., and Mendelssohn, M.J. (1991) A computer simulation approach to modeling the structure, thermodynamics and oxygen isotope equilibria of silicates. Physics and Chemistry of Minerals, 17, 690–699.

Peacor, D.R. (1968) A high temperature single crystal diffractometer study of leucite, (K,Na)AlSi$_2$O$_6$. Zeitschrift für Kristallographie, 127, 213–224.

Phillips, B.L., Kirkpatrick, R.J., and Putnis, A. (1989) Si,Al ordering in leucite by high resolution ^{27}Al MAS NMR spectroscopy. Physics and Chemistry of Minerals, 16, 591–598.

Post, J.E., and Burnham, C.W. (1986) Ionic modeling of mineral structures and energies in the electron gas approximation: TiO$_2$ polymorphs, quartz, forsterite, diopside. American Mineralogist, 71, 142–150.

——— (1987) Structure-energy calculations on low and high albite. American Mineralogist, 72, 507–514.

Price, G.D., Parker, S.C., and Leslie, M. (1987) The lattice dynamics and thermodynamics of the Mg$_2$SiO$_4$ polymorphs. Physics and Chemistry of Minerals, 15, 181–190.

Putnis, A., Salje, E., Redfern, S.A.T., Fyfe, C.A., and Strobl, H. (1987) Structural states of Mg cordierite. I. Order parameters from synchrotron x-ray and NMR data. Physics and Chemistry of Minerals, 14, 446–454.

Salje, E.K.H. (1990) Phase transitions in ferroelastic and co-elastic crystals. 366 p. Cambridge University Press, Cambridge, U.K.

Salje, E., Kuscholke, B., Wruck, B., and Kroll, H. (1985) Thermodynamics of sodium feldspar. II. Experimental results and numerical calculations. Physics and Chemistry of Minerals, 12, 99–107.

Sanders, M.J., Leslie, M., and Catlow, C.R.A. (1984) Interatomic potentials for SiO$_2$. Journal of the Chemical Society, Chemical Communications, 1271–1273.

Winkler, B., Dove, M.T., and Leslie, M. (1991) Static lattice energy minimization and lattice dynamics calculations on aluminosilicate minerals. American Mineralogist, 76, 313–331.